Detecting electron neutrinos from solar dark matter annihilation by JUNO

Wan-Lei Guo*

Institute of High Energy Physics, Chinese Academy of Sciences,

P.O. Box 918, Beijing 100049, China

arXiv:1511.04888v3 [hep-ph] 27 Jan 2016

Abstract

We explore the electron neutrino signals from light dark matter (DM) annihilation in the Sun for the large liquid scintillator detector JUNO. In terms of the spectrum features of three typical DM annihilation channels $\chi\chi \to \nu\bar{\nu}, \tau^+\tau^-, b\bar{b}$, we take two sets of selection conditions to calculate the expected signals and atmospheric neutrino backgrounds based on the Monte Carlo simulation data. Then the JUNO sensitivities to the spin independent DM-nucleon and spin dependent DM-proton cross sections are presented. It is found that the JUNO projected sensitivities are much better than the current spin dependent direct detection experimental limits for the $\nu\bar{\nu}$ and $\tau^+\tau^-$ channels. In the spin independent case, the JUNO will give the better sensitivity to the DM-nucleon cross section than the LUX and CDMSlite limits for the $\nu\bar{\nu}$ channel with the DM mass lighter than 6.5 GeV. If the $\nu\bar{\nu}$ or $\tau^+\tau^-$ channel is dominant, the future JUNO results are very helpful for us to understand the tension between the DAMA annual modulation signal and other direct detection exclusions.

PACS numbers: 95.35.+d, 95.55.Vj, 13.15.+g

*Email:guowl@ihep.ac.cn

I. INTRODUCTION

The existence of dark matter (DM) is by now well confirmed [1, 2]. The current cosmological observations have helped to establish the concordance cosmological model where the present Universe consists of about 69.3% dark energy, 25.8% dark matter and 4.9% atoms [3]. Understanding the nature of dark matter is a prime open problem in particle physics and cosmology. Here we focus on the neutrino signals from the DM annihilation in the Sun. As well as in the DM direct detection experiments, the halo DM particles can also elastically scatter with nuclei in the Sun. Then they may lose most of their energy and are captured in the Sun [1]. These trapped DM particles will be accumulated in the core of the Sun due to repeated scatters and the gravity potential. Therefore the Sun is a very interesting place for us to search the DM annihilation signals. Due to the interactions of the DM annihilation products in the Sun, only the neutrino can escape from the Sun and reach the Earth. Therefore the terrestrial neutrino detectors can detect these neutrinos. The Cherenkov detectors Super-Kamiokande [4], IceCube [5] and ANTARES [6] have presented their results.

The Jiangmen Underground Neutrino Observatory (JUNO) [7], a 20 kton multi-purpose underground liquid scintillator (LS) detector, are constructing in China to primarily determine the neutrino mass hierarchy by detecting reactor antineutrinos. The JUNO central detector as a LS calorimeter has an excellent energy resolution and a very low energy threshold. It is found that the LS detector has capability to reconstruct the track direction of the energetic charged particle by use of the timing pattern of the first-hit on the photomultiplier tubes (PMTs) since the energetic particle travels faster than light in the LS [8, 9]. Therefore the JUNO LS detector can detect the neutrinos from the DM annihilation in the Sun. In Ref. [7], the JUNO has calculated the $\nu_\mu/\overline{\nu}_\mu$ signals from the DM annihilation in the Sun. Some authors have analyzed the $\nu_e/\overline{\nu}_e$ and $\nu_\mu/\overline{\nu}_\mu$ signals for the other LS detectors [10]. Here we shall discuss the $\nu_e/\overline{\nu}_e$ signals from the solar DM annihilation in JUNO.

In this paper, we shall explore the $\nu_e/\overline{\nu}_e$ signals in JUNO from the light DM annihilation $4\,\mathrm{GeV} \leq m_D \leq 20\,\mathrm{GeV}$ and consider three typical DM annihilation channels $\chi\chi \to \nu\overline{\nu}, \tau^+\tau^-, b\overline{b}$. Two sets of selection conditions will be chosen for the monoenergetic ($\nu\overline{\nu}$ channel) and continuous ($\tau^+\tau^-$ and $b\overline{b}$ channels) spectrum cases. Then we calculate the corresponding selection efficiencies and the atmospheric neutrino background based on the Monte Carlo (MC) simulation data. The JUNO sensitivities to the spin-independent (SI) DM-nucleon and spin-dependent (SD) DM-proton

elastic scattering cross sections will be given for the three DM annihilation channels. This paper is organized as follows: In Sec. II, we outline the main features of the DM captured by the Sun and give the produced neutrino fluxes. In Sec. III, we present the selection conditions and numerically calculate the corresponding $\nu_e/\bar{\nu}_e$ event numbers in JUNO. In Sec. IV, we analyze the expected atmospheric neutrino background and calculate the JUNO sensitivities to the DM direct detect cross sections. Finally, a conclusion will be given in Sec. V.

II. NEUTRINOS FROM THE DM ANNIHILATION IN THE SUN

A halo DM particle via elastic scattering with the solar nuclei may lose most of its energy and is trapped by the Sun [1]. On the other hand, each DM annihilation in the Sun will deplete two DM particles. The evolution of the DM number N in the Sun can be written as [11]:

$$\dot{N} = C_\odot - C_A N^2 \ , \tag{1}$$

where the dot denotes differentiation with respect to time. The DM solar capture rate $C_\odot$ in Eq. (1) is proportional to the DM-nucleon (DM-proton) elastic scattering cross section $\sigma_n^{\rm SI}$ ($\sigma_p^{\rm SD}$) in the SI (SD) interaction case. In the next paragraph, we shall give the corresponding formulas to calculate $C_\odot$. The last term $C_A N^2$ in Eq. (1) controls the DM annihilation rate in the Sun. The coefficient C_A depends on the the thermally averaged annihilation cross section times the relative velocity $\langle\sigma v\rangle$ and the DM distribution in the Sun. To a good approximation, one can obtain $C_A = \langle\sigma v\rangle/V_{eff}$, where $V_{eff} = 5.8\times10^{30}\ {\rm cm}^3(1{\rm GeV}/m_D)^{3/2}$ is the effective volume of the core of the Sun [11, 12]. In Eq. (1), we have neglected the evaporation effect since this effect is very small when the DM mass $m_D \gtrsim 4$ GeV [13]. One can easily solve the evolution equation and derive the DM solar annihilation rate [11]

$$\Gamma_A = \frac{1}{2}C_A N^2 = \frac{1}{2}C_\odot \tanh^2(t_\odot\sqrt{C_\odot C_A}) \ , \tag{2}$$

where $t_\odot \simeq 4.5$ Gyr is the solar age. If $t_\odot\sqrt{C_\odot C_A} \gg 1$, the DM annihilation rate reaches equilibrium with the DM capture rate. In the equilibrium case, one may derive the maximal DM annihilation rate $\Gamma_A = C_\odot/2$ which means that the DM annihilation signals will only depend on $\sigma_n^{\rm SI}$ or $\sigma_p^{\rm SD}$.

In the following parts, we shall use $C_\odot^{\rm SI}$ and $C_\odot^{\rm SD}$ to represent the solar capture rate $C_\odot$ in the SI

and SD interaction cases, respectively. $C_\odot^{\rm SI}$ and $C_\odot^{\rm SD}$ may be approximately written as [1]

$$C_\odot^{\rm SI} \approx 4.8\times10^{24}{\rm s}^{-1}\frac{\rho_0}{0.3\,{\rm GeV/cm}^3}\frac{270\,{\rm km/s}}{\bar{v}}\frac{1{\rm GeV}}{m_D}\sum_i F_i(m_D)\frac{\sigma_{N_i}^{\rm SI}}{10^{-40}{\rm cm}^2}f_i\phi_i S\left(\frac{m_D}{m_{N_i}}\right)\frac{1{\rm GeV}}{m_{N_i}}\,, \quad (3)$$

$$C_\odot^{\rm SD} \approx 1.3\times10^{25}{\rm s}^{-1}\frac{\rho_0}{0.3\,{\rm GeV/cm}^3}\frac{270\,{\rm km/s}}{\bar{v}}\frac{1{\rm GeV}}{m_D}\frac{\sigma_p^{\rm SD}}{10^{-40}{\rm cm}^2}S\left(\frac{m_D}{m_p}\right)\,, \quad (4)$$

where the local DM density $\rho_0 = 0.3\,{\rm GeV/cm}^3$ and the local DM root-mean-square velocity $\bar{v} = 270\,{\rm km/s}$. The function $S(x)$ denotes the kinematic suppression and is given by

$$S(x) = \left[\frac{A(x)^{1.5}}{1+A(x)^{1.5}}\right]^{2/3} \text{ with } A(x) = \frac{3x}{2(x-1)^2}\left(\frac{\langle v_{\rm esc}\rangle}{\bar{v}}\right)^2\,, \quad (5)$$

where $\langle v_{\rm esc}\rangle = 1156$ km s^{-1} is a mean escape velocity. f_i and ϕ_i describe the mass fraction and the distribution of the element N_i in the Sun, respectively. f_i, ϕ_i and the form-factor suppression $F_i(m_D)$ can be found in Ref. [1]. We shall sum over the following elements in the Sun: ^{1}H, ^{4}He, ^{12}C, ^{14}N, ^{16}O, ^{20}Ne, ^{24}Mg, ^{28}Si, ^{32}S and ^{56}Fe. The SI DM-nucleus elastic scattering cross section $\sigma_{N_i}^{\rm SI}$ is related to the SI DM-nucleon elastic scattering cross section $\sigma_n^{\rm SI}$ by the formula [14]

$$\sigma_{N_i}^{\rm SI} = A_{N_i}^2\frac{M^2(N_i)}{M^2(n)}\sigma_n^{\rm SI}\,, \quad (6)$$

where A_{N_i} is the mass number of the nucleus N_i and $M(x) = m_D m_x/(m_D+m_x)$. Here we have assumed that the DM couplings to protons and neutrons are isospin-invariant. Assuming $\sigma_n^{\rm SI} = \sigma_p^{\rm SD} = 10^{-40}$ cm^2, we calculate $C_\odot^{\rm SI}$ and $C_\odot^{\rm SD}$ as shown in Fig. 1. It is found that $C_\odot^{\rm SI}$ from other elements in the Sun is much larger than that from the hydrogen element although it has the maximal mass fraction. In the SD case, the hydrogen element plays the dominant role.

Considering the usual $\langle\sigma v\rangle \approx 3\times10^{-26}$ cm^3 s^{-1} induced from the observed DM relic density, we can obtain $C_\odot \geq 8.6\times10^{22}/(m_D/1{\rm GeV})^{3/2}{\rm s}^{-1}$ [15] from $t_\odot\sqrt{C_\odot C_A} \geq 3.0$ which means $\tanh^2[t_\odot\sqrt{C_\odot C_A}] \geq 0.99$ in Eq. (2). In terms of the results in Fig. 1, we may safely assume that the DM annihilation rate reaches equilibrium with the DM capture rate. Then the electron neutrino flux at the surface of the Earth from the solar DM annihilation can be written as:

$$\frac{d\Phi_{\nu_e}}{dE_\nu} = \frac{\Gamma_A}{4\pi R_{\rm ES}^2}\frac{dN_{\nu_e}}{dE_\nu} \simeq \frac{C_\odot}{8\pi R_{\rm ES}^2}\frac{dN_{\nu_e}}{dE_\nu}\,, \quad (7)$$

where $R_{\rm ES} = 1.496\times10^{13}$ cm is the Earth-Sun distance. dN_{ν_e}/dE_ν is the differential electron neutrino energy spectrum from per DM pair annihilation in the Sun. In order to calculate dN_{ν_e}/dE_ν, one must consider the hadronization, interactions and decay processes of the DM annihilation final

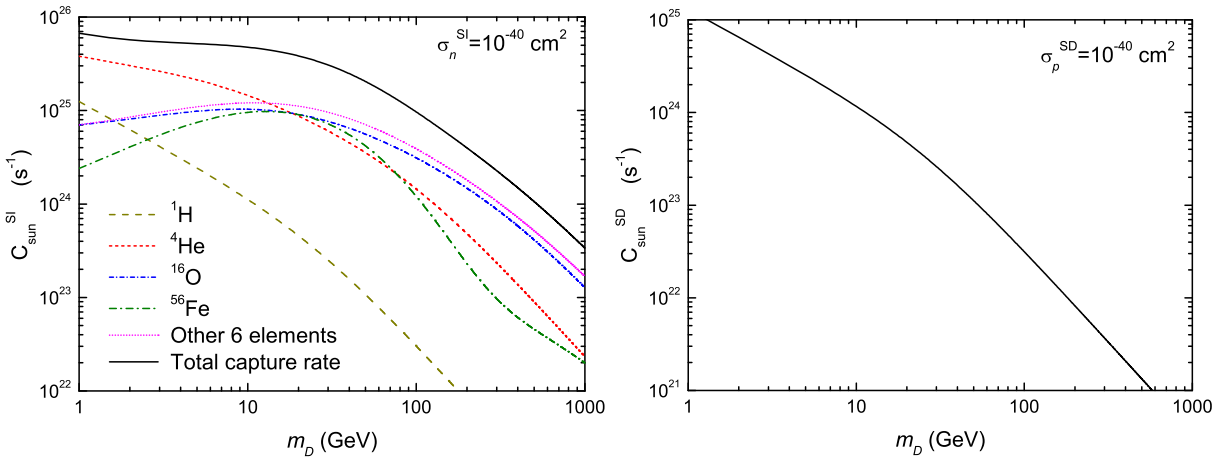

FIG. 1: The DM solar capture rates $C_\odot^{\rm SI}$ (left) and $C_\odot^{\rm SD}$ (right) as a function of m_D with $\sigma_n^{\rm SI} = \sigma_p^{\rm SD} = 10^{-40}$ cm^2. The related contributions to $C_\odot^{\rm SI}$ from ^{1}H, ^{4}He, ^{16}O, ^{56}Fe and other 6 elements have also been shown.

states in the core of the Sun. In addition, we should consider the neutrino interactions in the Sun and neutrino oscillations. Here the following neutrino oscillation parameters will be chosen as input values: [16, 17]

$$\begin{aligned} \sin^2\theta_{12} &= 0.308, \quad \sin^2\theta_{23} = 0.437, \quad \sin^2\theta_{13} = 0.0234, \\ \Delta m^2_{21} &= 7.54\times10^{-5}\text{eV}^2, \quad \Delta m^2_{31} = 2.47\times10^{-3}\text{eV}^2, \quad \delta = 0^\circ. \end{aligned} \tag{8}$$

Then we use the program package WimpSim [18] to calculate dN_{ν_e}/dE_ν and $dN_{\bar{\nu}_e}/dE_\nu$ for three typical DM annihilation channels $\chi\chi \to \nu\bar{\nu}, \tau^+\tau^-, b\bar{b}$ and 4 GeV $\leq m_D \leq$ 20 GeV. Note that $\nu_e\bar{\nu}_e$, $\nu_\mu\bar{\nu}_\mu$ and $\nu_\tau\bar{\nu}_\tau$ have the same contributions in the $\nu\bar{\nu}$ channel.

III. ELECTRON NEUTRINOS AND ANTINEUTRINOS IN JUNO

Here we shall discuss the $\nu_e/\bar{\nu}_e$ signals in JUNO from the DM $\nu\bar{\nu}$, $\tau^+\tau^-$ and $b\bar{b}$ annihilation channels. The JUNO central detector holds 20 kton LS which will be in a spherical container of radius of 17.7 m [7]. There is 1.5 m water buff region between about 17000 20-inch PMTs and the LS surface. According to the detector properties, we have made a MC simulation based on the GENIE generator [19] and the Geant4 detector simulation [20]. For the $\nu_e/\bar{\nu}_e$ charged current (CC) interactions in the JUNO detector, the MC simulation can provide many useful information which includes the event visible energy E_{vis}, the $e^\pm$ visible energy E^e_{vis}, the initial neutrino direction, the final state $e^\pm$ direction, etc.

The JUNO can reconstruct E_{vis} with a very excellent energy resolution $\sigma_{E_{vis}}$. For the $\nu_e/\bar{\nu}_e$ from

4 – 20 GeV DM annihilation, we may conservatively take $\sigma_{E_{vis}} = 0.01\sqrt{E_{vis}/\mathrm{GeV}}$ which origins from the statistical fluctuation in the scintillation photon emission and the quenching fluctuation [7]. The $\sigma_{E_{vis}}$ will be neglected in the following analysis since it has the very slight effects. On the other hand, the JUNO can also reconstruct the single muon direction with the angular resolution better than 1° if its track length $L_\mu > 5$ m and intrinsic PMT timing resolution better than 4 ns [7]. For the single electron/positron track, the 50 kton LS detector LENA find that the angular resolution is a few degrees [9]. Note that the hadronic final states in the ν_e and $\bar{\nu}_e$ CC interactions will affect the $e^\pm$ angular resolution and the identification of electron shower. The related studies are under way. Here we assume the $\nu_e/\bar{\nu}_e$ CC events with $E^e_{vis} > 1$ GeV and $Y_{vis} \equiv E^e_{vis}/E_{vis} > 0.5$ can be identified and reconstructed very well. For these selected events, the $e^\pm$ angular resolution will be assumed to be 10° in the following analysis.

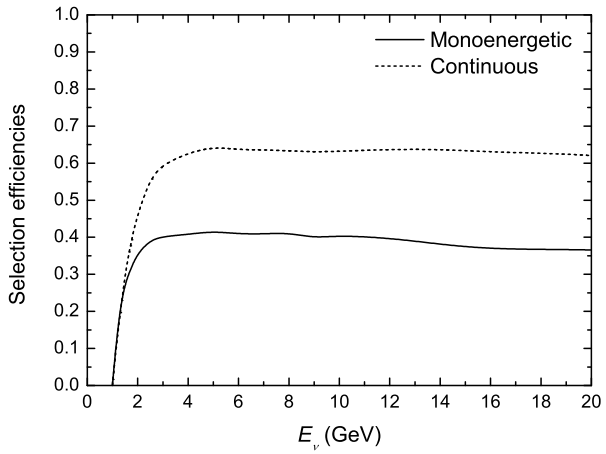

FIG. 2: The $\nu_e/\bar{\nu}_e$ CC event selection efficiencies $\epsilon(E_\nu)$ as a function of initial neutrino energy E_ν based on the corresponding selection conditions in the monoenergetic and continuous spectrum cases.

For the DM $\nu\bar{\nu}$ annihilation channel, the WimpSim gives an approximate monoenergetic $\nu_e/\bar{\nu}_e$ spectrum. This is because that the initial monoenergetic $\nu_e/\bar{\nu}_e$ spectrum ($E_\nu = m_D$) will be slightly modified by the neutrino interactions in the Sun. The DM $\tau^+\tau^-$ and $b\bar{b}$ annihilation channels have the continuous spectra. In order to suppress the atmospheric neutrino backgrounds, we shall take different selection conditions for a given $\nu_e/\bar{\nu}_e$ energy E_ν in the monoenergetic and continuous $\nu_e/\bar{\nu}_e$ spectrum cases. Then two selection efficiencies $\epsilon(E_\nu)$ will be obtained from the MC simulation data. Except for $E^e_{vis} > 1$ GeV and $Y_{vis} \equiv E^e_{vis}/E_{vis} > 0.5$, we only select the events with $\theta_{\rm sun} < 20^\circ\sqrt{10\mathrm{GeV}/E_\nu}$ [1] and $1 \geq E_{vis}/E_\nu > 0.9$ for the monoenergetic spectrum case. Here $\theta_{\rm sun}$

denotes the angle between the initial neutrino direction (the Sun direction) and the reconstructed $e^{\pm}$ direction. Based on the $e^{\pm}$ initial direction and 10° angular resolution, one can easily calculate the angle $\theta_{\rm sun}$ for every MC simulation event. For the continuous spectrum case, $E^{e}_{vis} > 1$ GeV, $Y_{vis} > 0.5$, $\theta_{\rm sun} < 30°$ and $1\,{\rm GeV} < E_{vis} < E_{\nu}$ will be chosen. Then we calculate the corresponding selection efficiencies $\epsilon(E_{\nu})$ for a given energy $\nu_e/\bar{\nu}_e$ in the monoenergetic and continuous spectrum cases as shown in Fig. 2. It is found that $\epsilon(E_{\nu})$ will not obviously change for $E_{\nu} > 3$ GeV.

For a given DM mass m_D, the expected $\nu_e/\bar{\nu}_e$ CC event numbers from the DM annihilation in the Sun can be expressed as

$$N_S = N_n\, t \int_{E_{th}}^{m_D} \left[\frac{d\Phi_{\nu_e}}{dE_{\nu}} \sigma_{\nu_e} + \frac{d\Phi_{\bar{\nu}_e}}{dE_{\nu}} \sigma_{\bar{\nu}_e} \right] \epsilon(E_{\nu})\, dE_{\nu} \,, \tag{9}$$

where the total nucleon number $N_n \simeq 20\,{\rm kton}/m_n$ and m_n is the nucleon mass. In the following parts, we shall take the JUNO exposure time $t = 10$ years. Here we extract ν_e ($\bar{\nu}_e$) per nucleon CC cross section σ_{ν_e} ($\sigma_{\bar{\nu}_e}$) from the GENIE [19] and consider that the LS target includes 12% ^{1}H and 88% ^{12}C. σ_{ν_e} and $\sigma_{\bar{\nu}_e}$ can also be found in the left panel of Fig. 7-5 in Ref. [7]. In Eq. (9), the integral lower limit $E_{th} = 0.9 m_D$ ($E_{th} = 1$ GeV) for the DM $\nu\bar{\nu}$ channel ($\tau^+\tau^-$ and $b\bar{b}$ channels) will be chosen. With the help of Eq. (7), Eq. (9) and the efficiencies $\epsilon(E_{\nu})$ in Fig. 2, one can calculate the expected event numbers N_S for different DM masses and annihilation channels. For illustration, we plot N_S as a function of m_D in the left panel of Fig. 3 with $\sigma_n^{\rm SI} = 10^{-40}$ cm^2 and $\sigma_p^{\rm SD} = 10^{-40}$ cm^2.

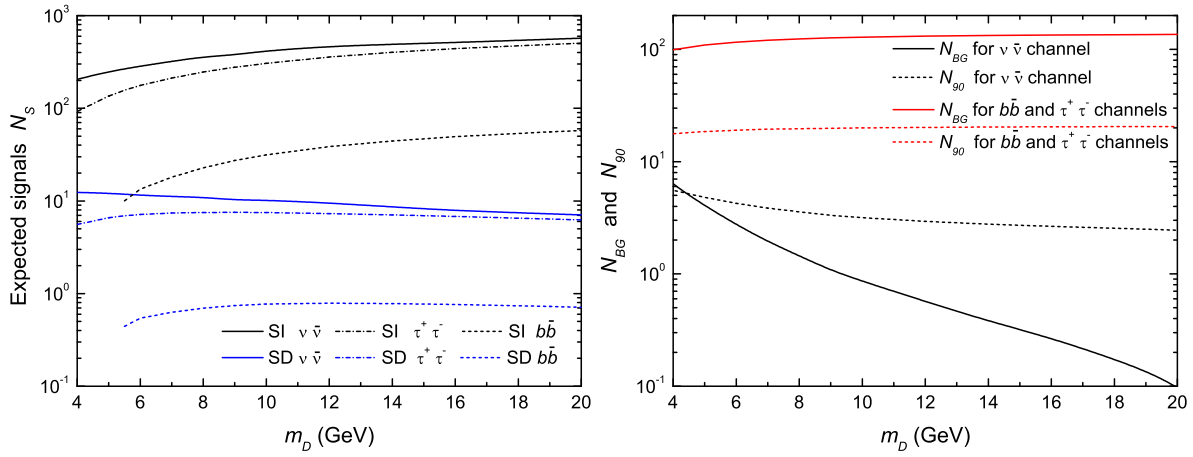

FIG. 3: Left panel: the expected signals N_S from the DM $\nu\bar{\nu}$, $\tau^+\tau^-$ and $b\bar{b}$ channels for the $\sigma_n^{\rm SI} = 10^{-40}$ cm^2 and $\sigma_p^{\rm SD} = 10^{-40}$ cm^2 cases. Right panel: the atmospheric $\nu_e/\bar{\nu}_e$ CC backgrounds N_{BG} and the deduced 90% CL upper limit N_{90} to N_S for the monoenergetic and continuous spectrum cases.

IV. SENSITIVITIES TO THE DM DIRECT DETECTION CROSS SECTIONS

For the $\nu_e/\bar{\nu}_e$ signals from the DM annihilation in the Sun, the related backgrounds are due to the atmospheric neutrino CC and neutral current (NC) interactions in the JUNO. The atmospheric $\nu_e/\bar{\nu}_e$ CC events are the irreducible background. The atmospheric neutrino NC background mainly origins from the π^0 misidentification as $e^{\pm}$. As shown in Fig. 7-5 of Ref. [7], the NC event rate is about half of the $\nu_e/\bar{\nu}_e$ CC event rate for $E_{vis} > 1$ GeV. Note that the $e^{\pm}$ takes on average about 60% of the initial $\nu_e/\bar{\nu}_e$ energy in the CC interaction. For the NC interaction, several hadronic particles will usually share E_{vis}. Considering the requirement $E^e_{vis} > 1$ GeV and the π^0 misidentification rate, we shall neglect the atmospheric neutrino NC background and only calculate the atmospheric $\nu_e/\bar{\nu}_e$ CC background.

With the help of the GENIE generator and Geant4 detector simulation, 1.5 million $\nu_e/\bar{\nu}_e$ CC events in JUNO detector have been simulated [7]. On the other hand, we calculate the expected atmospheric $\nu_e/\bar{\nu}_e$ CC event numbers in every energy and zenith angle bin by use of the atmospheric neutrino fluxes [21] and the oscillation parameters in Eq. (8). Comparing the event numbers per bin of the MC simulation and the corresponding theoretical values, we determine the weight value for every MC event. Then the expected atmospheric $\nu_e/\bar{\nu}_e$ CC sample can be obtained. For the DM $\nu\bar{\nu}$ channel, we apply the selection conditions $E^e_{vis} > 1$ GeV, $Y_{vis} > 0.5$ and $1 \geq E_{vis}/m_D > 0.9$ to calculate the corresponding atmospheric $\nu_e/\bar{\nu}_e$ CC event numbers from all directions. Then we average the all direction result and obtain the atmospheric $\nu_e/\bar{\nu}_e$ CC background N_{BG} within the cone half-angle $\theta_{\rm sun} < 20^\circ \sqrt{10{\rm GeV}/m_D}$. For the $\tau^+\tau^-$ and $b\bar{b}$ channels, $E^e_{vis} > 1$ GeV, $Y_{vis} > 0.5$, $1\,{\rm GeV} < E_{vis} < m_D$ and $\theta_{\rm sun} < 30^\circ$ will be used. In the right panel of Fig. 3, we plot the atmospheric $\nu_e/\bar{\nu}_e$ CC background N_{BG} as a function of m_D. It is clear that the $\nu\bar{\nu}$ channel has the smaller N_{BG} than the $\tau^+\tau^-$ and $b\bar{b}$ channels. This is because that we take $1\,{\rm GeV} < E_{vis} < m_D$ and a larger cone half-angle $\theta_{\rm sun}$ for the DM $\tau^+\tau^-$ and $b\bar{b}$ channels.

To estimate the JUNO sensitivities to the direct detection cross sections $\sigma_n^{\rm SI}$ and $\sigma_p^{\rm SD}$, we assume the observed event number $N_{obs} = N_{BG}$. Then the 90% confidence level (CL) upper limit N_{90} to the expected $\nu_e/\bar{\nu}_e$ signals N_S can be derived through the following formulas [4]:

$$90\% = \frac{\int_{N_S=0}^{N_{90}} L(N_{obs}|N_S)dN_S}{\int_{N_S=0}^{\infty} L(N_{obs}|N_S)dN_S} \tag{10}$$

with the Poisson-based likelihood function

$$L(N_{obs}|N_S) = \frac{(N_S + N_{BG})^{N_{obs}}}{N_{obs}!} e^{-(N_S+N_{BG})} \ . \tag{11}$$

In terms of N_{BG}, we calculate the corresponding upper limit N_{90} for the $\nu\bar{\nu}$, $\tau^+\tau^-$ and $b\bar{b}$ channels. In the right panel of Fig. 3, we plot N_{90} as a function of m_D. It is found that N_{90} decreases from 5.6 to 2.5 as the DM mass m_D increases in the $\nu\bar{\nu}$ channel case. For the $\tau^+\tau^-$ and $b\bar{b}$ channels, N_{90} only slightly changes.

The JUNO sensitivities to $\sigma_n^{\rm SI}$ and $\sigma_p^{\rm SD}$ can be derived from $N_S = N_{90}$ and Eq. (9). In Fig. 4, we plot the JUNO sensitivities as a function of m_D for the DM $\nu\bar{\nu}$, $\tau^+\tau^-$ and $b\bar{b}$ channels with 10 year running. Here the current experimental results from the direct detection experiments have also been shown. Note that DAMA/LIBRA [22, 23], CDMS-Si [24], CoGeNT [25] and CRESST-II [26, 27] have the positive results which can be interpreted as arising from the SI DM-nucleon interaction with the shadowed parameter space [24] as shown in the left panel of Fig. 4. However the LUX [28], XENON100 [29], CDMSlite [30], SuperCDMS [31] and CDEX-1 [32] experiments do not find the DM evidence and only give the upper limits to $\sigma_n^{\rm SI}$. It is clear that the JUNO projected sensitivity to $\sigma_n^{\rm SI}$ is better than the direct detection experiments for the $\nu\bar{\nu}$ channel with $m_D < 6.5$ GeV. If the $\nu\bar{\nu}$ or $\tau^+\tau^-$ channel is dominant, the future JUNO results are very helpful for us to understand the tension between the DAMA annual modulation signal and other direct detection exclusions. In the SD case, the JUNO sensitivities to $\sigma_p^{\rm SD}$ from the $\nu\bar{\nu}$ and $\tau^+\tau^-$ channels are much better than the current PICO-2L [33], PICASSO [34] and SIMPLE-II [35] experimental limits.

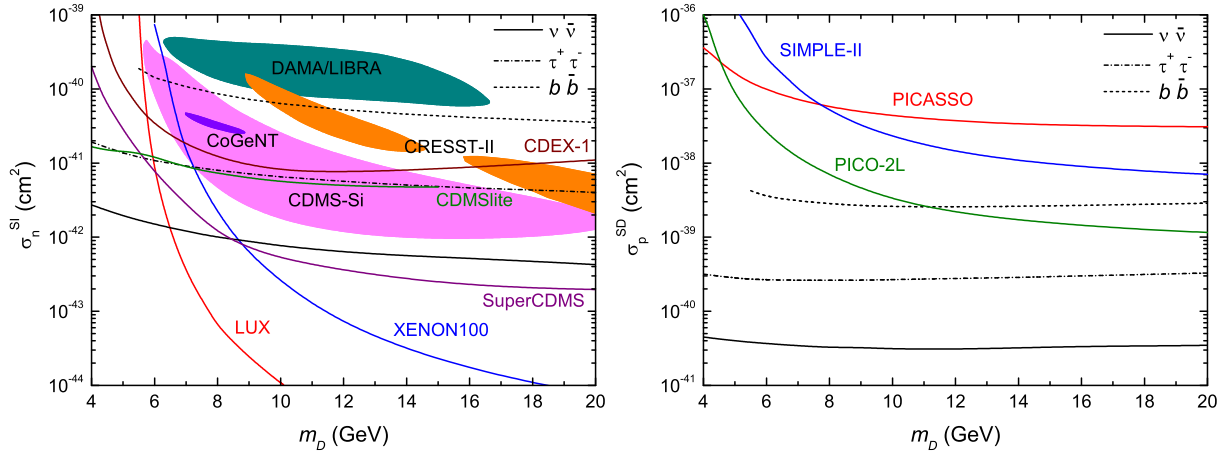

FIG. 4: The JUNO sensitivities to $\sigma_n^{\rm SI}$ (left) and $\sigma_p^{\rm SD}$ (right) as a function of m_D for the DM $\nu\bar{\nu}$, $\tau^+\tau^-$ and $b\bar{b}$ annihilation channels with 10 year data.

V. CONCLUSIONS

In conclusion, we have investigated the ν_e and $\bar{\nu}_e$ CC signals in JUNO from the DM annihilation in the Sun. Three typical DM annihilation channels $\chi\chi \to \nu\bar{\nu}, \tau^+\tau^-, b\bar{b}$ have been analyzed for the light DM mass 4 GeV $\leq m_D \leq$ 20 GeV. In terms of the spectrum features, we take two sets of selection conditions for the monoenergetic ($\nu\bar{\nu}$ channel) and continuous ($\tau^+\tau^-$ and $b\bar{b}$ channels) spectra. The corresponding selection efficiencies $\epsilon(E_\nu)$ can be derived for a given $\nu_e/\bar{\nu}_e$ energy from the MC simulation data and 10° angular resolution. Then we numerically calculate the expected ν_e and $\bar{\nu}_e$ CC event numbers for the SI and SD interactions. On the other hand, we calculate the irreducible atmospheric $\nu_e/\bar{\nu}_e$ CC background which is far larger than the atmospheric neutrino NC background. Finally, we present the JUNO sensitivities to $\sigma_n^{\rm SI}$ and $\sigma_p^{\rm SD}$ for the DM $\nu\bar{\nu}$, $\tau^+\tau^-$ and $b\bar{b}$ annihilation channels with 10 year running. It is found that the JUNO projected sensitivities to $\sigma_p^{\rm SD}$ are much better than the current experimental upper limits for the $\nu\bar{\nu}$ and $\tau^+\tau^-$ channels. For the SI case, the JUNO will give the better sensitivity to $\sigma_n^{\rm SI}$ than the current direct detection experiments for $m_D < 6.5$ GeV in the $\nu\bar{\nu}$ channel case.

Acknowledgments

I am grateful to Tao Lin and Jia-Shu Lu for their useful help in the Geant4 detector simulation and the GENIE generator. This work is supported in part by the National Nature Science Foundation of China (NSFC) under Grants No. 11575201 and the Strategic Priority Research Program of the Chinese Academy of Sciences under Grant No. XDA10010100.

[1] G. Jungman, M. Kamionkowski and K. Griest, Phys. Rept. **267**, 195 (1996).

[2] G. Bertone, D. Hooper and J. Silk, Phys. Rept. **405**, 279 (2005).

[3] P. A. R. Ade *et al.* [Planck Collaboration], arXiv:1502.01589 [astro-ph.CO].

[4] T. Tanaka *et al.* [Super-Kamiokande Collaboration], Astrophys. J. **742**, 78 (2011) [arXiv:1108.3384 [astro-ph.HE]]; K. Choi *et al.* [Super-Kamiokande Collaboration], Phys. Rev. Lett. **114**, no. 14, 141301 (2015) [arXiv:1503.04858 [hep-ex]].

[5] R. Abbasi *et al.* [IceCube Collaboration], Phys. Rev. D **85**, 042002 (2012) [arXiv:1112.1840 [astro-ph.HE]]; M. G. Aartsen *et al.* [IceCube Collaboration], Phys. Rev. Lett. **110**, no. 13, 131302 (2013)

[arXiv:1212.4097 [astro-ph.HE]]; arXiv:1510.05226 [astro-ph.HE].

[6] S. Adrian-Martinez *et al.* [ANTARES Collaboration], JCAP **1311**, 032 (2013) [arXiv:1302.6516 [astro-ph.HE]].

[7] F. An *et al.* [JUNO Collaboration], arXiv:1507.05613 [physics.ins-det].

[8] J. G. Learned, arXiv:0902.4009 [hep-ex]; J. Peltoniemi, arXiv:0909.4974 [physics.ins-det].

[9] M. Wurm *et al.* [LENA Collaboration], Astropart. Phys. **35**, 685 (2012) [arXiv:1104.5620 [astro-ph.IM]].

[10] J. Kumar, J. G. Learned and S. Smith, Phys. Rev. D **80**, 113002 (2009) [arXiv:0908.1768 [hep-ph]]; J. Kumar, J. G. Learned, M. Sakai and S. Smith, Phys. Rev. D **84**, 036007 (2011) [arXiv:1103.3270 [hep-ph]]; J. Kumar, J. G. Learned, S. Smith and K. Richardson, Phys. Rev. D **86**, 073002 (2012) [arXiv:1204.5120 [hep-ph]]; J. Kumar and P. Sandick, JCAP **1506**, no. 06, 035 (2015) [arXiv:1502.02091 [hep-ph]].

[11] K. Griest and D. Seckel, Nucl. Phys. B **283**, 681 (1987) [Erratum-ibid. B **296**, 1034 (1988)].

[12] A. Gould, Astrophys. J. **321**, 571 (1987).

[13] A. Gould, Astrophys. J. **321**, 560 (1987); D. Hooper, F. Petriello, K. M. Zurek and M. Kamionkowski, Phys. Rev. D **79**, 015010 (2009) [arXiv:0808.2464 [hep-ph]].

[14] W. L. Guo and Y. L. Wu, JHEP **1010**, 083 (2010) [arXiv:1006.2518 [hep-ph]]; Nucl. Phys. B **867**, 149 (2013) [arXiv:1103.5606 [hep-ph]].

[15] W. L. Guo, Z. L. Liang and Y. L. Wu, Nucl. Phys. B **878**, 295 (2014) [arXiv:1305.0912 [hep-ph]].

[16] F. Capozzi, G. L. Fogli, E. Lisi, A. Marrone, D. Montanino and A. Palazzo, Phys. Rev. D **89**, 093018 (2014) [arXiv:1312.2878 [hep-ph]].

[17] F. P. An *et al.* [DAYA-BAY Collaboration], Phys. Rev. Lett. **108**, 171803 (2012) [arXiv:1203.1669 [hep-ex]]; Chin. Phys. C **37**, 011001 (2013) [arXiv:1210.6327 [hep-ex]].

[18] J. Edsjo, WimpSim Neutrino Monte Carlo, http://copsosx03.fysik.su.se/wimpsim/; M. Blennow, J. Edsjo and T. Ohlsson, JCAP **0801**, 021 (2008) [arXiv:0709.3898 [hep-ph]].

[19] C. Andreopoulos, A. Bell, D. Bhattacharya, F. Cavanna, J. Dobson, S. Dytman, H. Gallagher and P. Guzowski *et al.*, Nucl. Instrum. Meth. A **614**, 87 (2010) [arXiv:0905.2517 [hep-ph]].

[20] S. Agostinelli *et al.* [GEANT4 Collaboration], Nucl. Instrum. Meth. A **506**, 250 (2003).

[21] M. Honda, M. S. Athar, T. Kajita, K. Kasahara and S. Midorikawa, Phys. Rev. D **92**, no. 2, 023004 (2015) [arXiv:1502.03916 [astro-ph.HE]].

[22] R. Bernabei *et al.* [DAMA and LIBRA Collaborations], Eur. Phys. J. C **67**, 39 (2010)

[arXiv:1002.1028 [astro-ph.GA]].

[23] C. Savage, G. Gelmini, P. Gondolo and K. Freese, JCAP **0904**, 010 (2009) [arXiv:0808.3607 [astro-ph]].

[24] R. Agnese *et al.* [CDMS Collaboration], Phys. Rev. Lett. **111**, no. 25, 251301 (2013) [arXiv:1304.4279 [hep-ex]].

[25] C. E. Aalseth *et al.* [CoGeNT Collaboration], Phys. Rev. D **88**, 012002 (2013) [arXiv:1208.5737 [astro-ph.CO]].

[26] G. Angloher *et al.*, Eur. Phys. J. C **72**, 1971 (2012) [arXiv:1109.0702 [astro-ph.CO]].

[27] A. Brown, S. Henry, H. Kraus and C. McCabe, Phys. Rev. D **85**, 021301 (2012) [arXiv:1109.2589 [astro-ph.CO]].

[28] D. S. Akerib *et al.* [LUX Collaboration], Phys. Rev. Lett. **112**, 091303 (2014) [arXiv:1310.8214 [astro-ph.CO]].

[29] E. Aprile *et al.* [XENON100 Collaboration], Phys. Rev. Lett. **109**, 181301 (2012) [arXiv:1207.5988 [astro-ph.CO]].

[30] R. Agnese *et al.* [SuperCDMS Collaboration], [arXiv:1509.02448 [astro-ph.CO]].

[31] R. Agnese *et al.* [SuperCDMS Collaboration], Phys. Rev. Lett. **112**, no. 24, 241302 (2014) [arXiv:1402.7137 [hep-ex]].

[32] Q. Yue *et al.* [CDEX Collaboration], Phys. Rev. D **90**, 091701 (2014) [arXiv:1404.4946 [hep-ex]].

[33] C. Amole *et al.* [PICO Collaboration], Phys. Rev. Lett. **114**, no. 23, 231302 (2015) [arXiv:1503.00008 [astro-ph.CO]].

[34] S. Archambault *et al.* [PICASSO Collaboration], Phys. Lett. B **711**, 153 (2012) [arXiv:1202.1240 [hep-ex]].

[35] M. Felizardo *et al.*, Phys. Rev. Lett. **108**, 201302 (2012) [arXiv:1106.3014 [astro-ph.CO]].